Identification of areas susceptible to calcium carbonate formation on the surface of a plate and gasket heat exchanger

Nihad Kamar, Marie Le Page Mostefa, Hervé Muhr, Pierre-Olivier Jost

Chemical Engineering Communications

ISSN: (Print) (Online) Journal homepage: https://www.tandfonline.com/loi/gcec20

Identification of areas susceptible to calcium carbonate formation on the surface of a plate and gasket heat exchanger

Nihad Kamar, Marie Le Page Mostefa, Hervé Muhr & Pierre-Olivier Jost

To cite this article: Nihad Kamar, Marie Le Page Mostefa, Hervé Muhr & Pierre-Olivier Jost (2022): Identification of areas susceptible to calcium carbonate formation on the surface of a plate and gasket heat exchanger, Chemical Engineering Communications, DOI: 10.1080/00986445.2022.2075741

To link to this article: https://doi.org/10.1080/00986445.2022.2075741

CHEMICAL ENGINEERING COMMUNICATIONS
https://doi.org/10.1080/00986445.2022.2075741

Identification of areas susceptible to calcium carbonate formation on the surface of a plate and gasket heat exchanger

Nihad Kamar[a], Marie Le Page Mostefa[a], Hervé Muhr[a], and Pierre-Olivier Jost[b]

[a]Reactions and Process Engineering Laboratory (LRGP), University of Lorraine, Nancy, France; [b]Sofchem, Rueil Malmaison, France

ABSTRACT

This study aims at inhibiting the formation of calcium carbonate in heat exchangers by using guided ultrasonic waves associated with the heterodyne effect of multiple frequencies. To provide a proof of concept, an experimental approach on a plate and joint heat exchanger was considered and complemented by a modeling approach. This study explains how to identify areas susceptible to calcium carbonate deposition. The scaled surface is analyzed using a 3 D digital microscope, the preferential deposition areas are identified and the fraction of the surface occupied by calcium carbonate is determined. In addition, modeling was performed to detect areas sensitive to temperature and fluid flow. The modeling was validated using experimental data from a scaled plate analyzed with a 3 D microscope. As a predictive tool, this model could be particularly useful in identifying effective strategies to mitigate or even eliminate fouling.

KEYWORDS

Calcium carbonate crystallization; comsol multiphysics modeling; fouling of heat exchangers; ultrasonic system; 3D digital microscope

Introduction

Fouling is defined as the formation of unwanted deposits on heat transfer surfaces that impede heat transfer (Pau et al. 2019). There are different forms of fouling, Epstein classified these forms into three major families, fouling by biological growth, sedimentation, and fouling by chemical reaction (Epstein 1983).

Fouling layers on the internal surfaces increase with time during the use of the heat exchanger (Ch 2010). These fouling layers have a lower thermal conductivity than the fluids or the conduction wall, so they increase the overall thermal resistance. Thus, the thermal efficiency of the heat exchangers will be reduced, a degradation of the thermo-hydraulic performance will also be observed over time, and the energy consumption will be increased (Ch 2010).

Current methods of treating heat exchanger fouling, whether chemical or mechanical, consist of either pre-dimensioning the exchanger or applying treatments during its operation (De, Grenoble, and Legay 2012).

Increasing costs of cleaning products, additional energy costs, and production downtime have contributed to the growing interest in controlling fouling (Müller-Steinhagen 2011). The total costs associated with fouling for the major industrialized countries are estimated to be over 4.4 billion dollars annually (Al-Haj Ibrahim 2012). In 1980, Thackery estimated that for every raw product, there is an additional cost of about 0.3% related to fouling (Thackery and Thackery 1980). Because of this, economic considerations should be among the most influential parameters in determining appropriate fouling allowances.

More recently, environmental legislation has put additional pressure on CO_2 emissions related to soiling and the use of cleaning chemicals (Müller-Steinhagen 2011).

Besides the fact that they can damage the equipment when performed mechanically (Pau and al. 2019), cleaning operations are believed to be expensive, and have a high environmental impact. However, there are other alternatives based on the use of ultrasonic waves for example (Pau et al. 2019).

CONTACT Nihad Kamar nihad.kamar@univ-lorraine.fr Reactions and Process Engineering Laboratory (LRGP), University of Lorraine, UMR 7274 CNRS, 1 rue Grandville BP20451, 54001 Nancy, France.

Other methods have recently emerged for mechanical self-cleaning of heat exchangers during operation. These systems use temperature outputs in a simulation and a Digital Twin controller to identify when fouling is occurring and trigger a cleaning response. However, these methods do not completely stop fouling. And even the final cleaning decision is made autonomously based on the condition of the equipment through intelligent systems are needed to automatically recognize the fouling that has occurred and take action to eliminate the fouling without human intervention. But these systems are still complex to implement, and with high water demand (Brooks and Roy 2022).

Several scientific studies have reported on the application of ultrasound to limit the occurrence of fouling (Habibi et al. 2016), and others have highlighted the intensification of heat transfer by the acoustic current generated by ultrasound (Wu and Ro 2005) (Tajik et al. 2013) (Bulliard-sauret 2016). This preventive treatment has an effect on the fouling surface rather than on the water quality.

However, all methods to reduce fouling require some understanding of the deposition mechanisms, structure, and adhesion of deposits on heat transfer surfaces (Müller-Steinhagen 2011).

To provide a proof of concept, an experimental approach on a plate and gasket heat exchanger was considered and completed by a modeling approach. It is important to identify the areas sensitive to calcium carbonate deposition in order to choose the best position for the ultrasonic system. The scaled surface was analyzed with a 3 D digital microscope, the preferred deposition areas were identified and the fraction of surface occupied by calcium carbonate was determined. In addition, modeling with the Heat Transfer module of Comsol Multiphysics was performed to detect the temperature and fluid flow-sensitive areas. The modeling is validated using experimental data from a scaled plate and analyzed with a 3 D microscope.

On the same approach, GSM Martins et al. performed another study on the structural analysis of two-plate and joint heat exchangers, the authors analyzed the exchanger plates numerically using the Static Structural module present in ANSYS 18. And experimentally using triaxial strain gauges to study the mechanical stresses and heat distribution zones for both types of plates (Martins et al. 2022). However, to our knowledge, no study has yet been published describing a general approach using numerical modeling and 3 D digital microscope analysis of a scaled plate to study the deposition distribution and detect areas susceptible to scale formation.

Indeed, it is difficult to obtain detailed information on the internal geometrical characteristics of a heat exchanger plate during operation. In some cases, especially for non-removable heat exchangers, this seems impossible. Numerical simulation is a method that gives access to detailed results at any point of the case studied. The capability of numerical methods has been verified in various engineering fields, such as heat transfer (Zhang et al. 2018), energy (Sakkaki et al. 2020), nanotechnology (Jakati, Balavalad, and Sheeparamatti 2016), optics (Singh and Kaler 2018). The integrated modules in Comsol Multiphysics provide a user-friendly environment to study all physical phenomena inside the exchanger during its operation.

In order to facilitate this study, a comparison of the experimental distribution of the mineral deposit and the temperature sensitive zones using a numerical simulation has been performed.

This will allow observing if there is an overlap between the most scaled areas of the plate and the most temperature sensitive areas.

This study is expected to fill the current gap in the understanding of mineral scaling in plate and gasket heat exchangers. The objective of this paper is to describe a general approach using numerical modeling and a 3 D digital microscope analysis of a scaled plate to study the distribution of the deposit and to detect the areas sensitive to scale formation.

Materials and methods

Heat exchanger

To study the scaling phenomenon in cooling circuits, 100 liters of water from the urban network, with scaling power, was heated up to 50 °C in a plate and gasket heat exchanger. After three days

Table 1. Thermal and hydrodynamic characteristics of the two circuits of the exchanger.

Hot circuit			Cold circuit	
Type of fluid	Demineralized water		Scaling water	
Temperature (°C)	Th, Inlet = 46.7	Th, Outlet =31.5	Tc, Inlet = 15.6	Tc, Outlet = 23.3
Volume flow (L. min^{-1})	16		1.67	
Flow velocity (m. s^{-1})	0.08		0.01	
Heat flux (W)	16869		899	
Reynolds number	390.5		41.1	

of operation, the exchanger was completely emptied and then dismantled to analyze the distribution of the deposit within the cold circuit. Table 1 shows the operating conditions of the two circuits during the test.

The characteristics of the cold water :

- Langelier Saturation Index (LSI) = 1 (Tends to scale if LSI greater than 0. However, experts recommend values between 1.5 and 2.5 before issuing a scale warning, according to the Quebec Ministry of the Environment and Climate Change).
- Ryznar Stability Index (RSI) = 5.8 (Tends to scale if RSI is less than 6.2, according to the Quebec Ministry of the Environment and Climate Change).

Heat exchanger plate

The scanned plate is a plate of a plate and gasket heat exchanger (Barriquand), model BAS*32*381*C*P11. And which is characterized by a particular design inside, have the main purpose of increasing turbulence and ensuring mechanical rigidity by a large number of metal-to-metal contacts. And also chevron splines inclined at an angle α ($\alpha = 60°$) to the main direction of flow.

The plate used has circular openings at their corners, which after assembly, allowed fluid flow between several plates. Nitrile gaskets, just clipped and not glued, ensure the sealing between the plates during the assembly and allow or not the circulation of fluids between them. Table 2 shows the technical characteristics of the plate.

The geometry of the plate and the seal (in Steep format) used during the 3 D digital microscope scan are shown in Figure 1.

To simplify the study, two geometries were created in two Comsol Multiphysics modules. One geometry represents the plate with the four inputs/outputs, and the other represents a longitudinal section of the plate.

Table 2. Dimensional characteristics of the plate.

Composition	316 steel
Seal	Nitrile
Width (mm)	139
Thickness (mm)	0.5
Length (mm)	450
Grooves	Obtuse shape
Spline angle (°)	60

Analytical techniques

The amount of deposit per gram/day/ unit area was calculated with and without ultrasonic treatment by dissolving the deposit with diluted 2% nitric acid, the determination of calcium and magnesium concentration was performed by using ICP-OES spectroscopy.

The nature of the deposit was identified by using RAMAN spectroscopy and the results were confirmed by SEM imaging and EDX probe.

The size of the crystals obtained was determined by a laser granulometry. The thickness of the deposit was analyzed by a 3 D digital microscope. All the results obtained are in the process of being published.

Available modules – COMSOL multiphysics

To understand the scaling phenomenon in a heat exchanger, two models were generated using Comsol Multiphysics version 5.6 software. Two similar studies are available in the Comsol platform (Application ID: 252; COMSOL 2021) and (Application ID: 99521 (COMSOL n.d.)).

Comsol was used to model the temperature fields and heat flows through the plates of a heat exchanger (COMSOL n.d.). To examine the actual behavior of the system, the modeling results were subsequently compared with the experimental results.

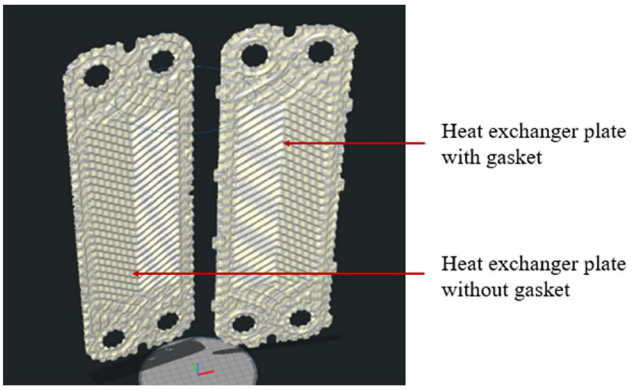

Figure 1. Heat exchanger plate with and without seal scanned.

Model of the exchanger plate

This model shows how to use the heat transfer and flow regime functionalities to understand the temperature distribution across the plate. This leads to a better understanding of the distribution of scale inside the exchanger.

- *Geometry*

Before doing any modeling/simulation, the cross-sectional selection of a representative geometry is considered. In case of absence, as in the case of this study, a 2 D scan by image assembly with a 3 D digital microscope allows to recover the geometry with medium accuracy, after a transformation of the image data into a point cloud in matrix format and then transforms it into X, Y, Z coordinates. The set of models is allowed to reconstruct a 3 D geometry of the plate. Given the precision and size of the latter, unfortunately, the Comsol model cannot be simulated. Therefore, a representative geometry was drawn on the Comsol, a rectangle of the same size as the real plate, with four holes that represent the inlet and outlet of the fluids.

Two domains were created above and below the plate, with a 6 mm spacing between each plate. This represents two chambers, one for the hot fluid and one for the cold fluid that exchanges heat through the middle plate, not counting the impact of nitrile seals, as shown in Figure 2.

It is possible to model the joints by using the Nascimento approach (Martins et al. 2022) but to reduce the computational cost the geometry of the plate has been designated without joints.

In this case, the heat transfer and fluid flow phenomena take place in the space between two plates, which corresponds to the cold compartment of the exchanger.

Note that the mesh applied to the geometry was a physics-controlled mesh. This type of mesh allows the model to be solved correctly and avoid convergence problems.

Definition of the model

The conditions of this model are as follows: the flow is laminar the inlet temperatures of the cold and hot fluids are 20 °C and 50 °C, respectively.

Model of the longitudinal section

This model focuses on the heat transfer between two superimposed sinusoidal plates, between which the water of the cold compartment circulates.

- *Geometry*

The 2 D geometry was drawn in Comsol Multiphysics version 5.6. It represents the stacking of two plates, about 260 mm long, with the splines 2 mm deep and a space between the plates of 6 mm. The principle is shown in Figure 3.

Note that the mesh applied to the geometry is a physics-controlled mesh, this will generate a correct mesh.

- *Definition of the model*

The conditions of this model are as follows: the inlet temperatures of the cold and hot fluids are respectively 20 °C and 50 °C; the fluid velocity is 0.01 (m/s).

- *Features of the Comsol Multiphysics integrated study*

The temperature of the cold liquid $T_{c,\ output}$ at the outlet has been calculated by the following relation which has been integrated into with COMSOL Multiphysics is

$$T_{c,out} = \frac{\int_{out} \rho.C_p.T.(\mathbf{u}\cdot\mathbf{n})}{\int_{out} \rho.C_p.(\mathbf{u}\cdot\mathbf{n})} \approx 40°C \qquad (1)$$

where C_p, the mass heat capacity in J kg^{-1} K^{-1}; ρ is the the density in kg m^{-3}; T is the

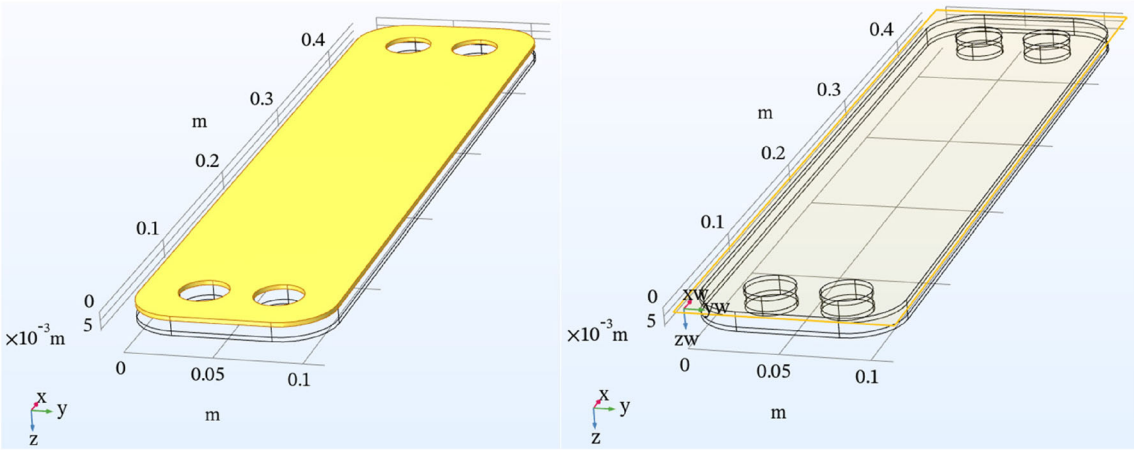

Figure 2. Simplified 3D geometry of the plate.

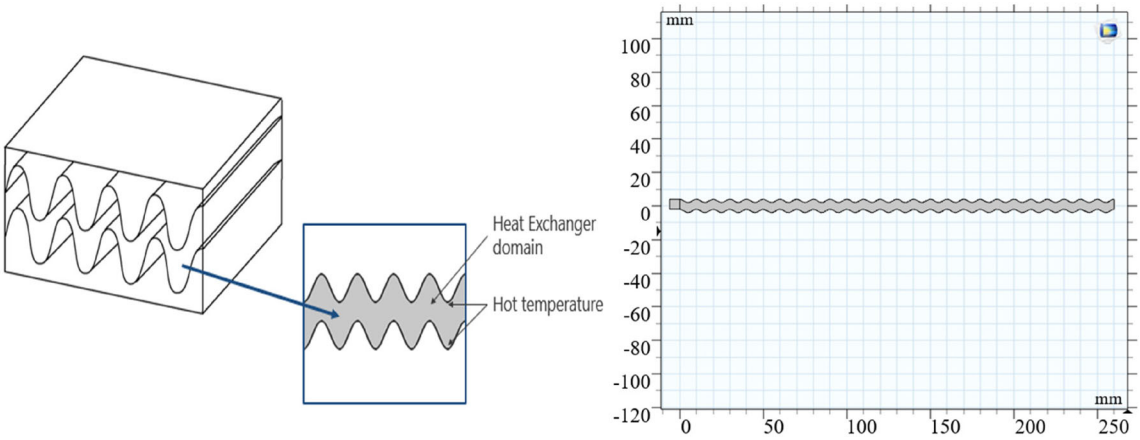

Figure 3. 2 D geometrical the second model of the stacking of two plates.

temperature in °C; u is the fluid velocity field in ms^{-1} and n is the unit vector.

And the overall exchange coefficient was calculated by the following relationship which has been integrated into Comsol multiphysics as well:

$$h_{eq} = \frac{P}{A.(T_{wall} - T_{in})} \approx 714 \ \mathrm{W/(m \cdot K)} \qquad (2)$$

h_{eq} is the global exchange coefficient in W m^{-2} K^{-1}, P is thermal power exchanged in W, and A is the exchange surface in m^2.

Microscope digital 3 D

The analysis of the scaled plates was performed with the VHX-7000 series 3 D digital microscope. This allows us to capture high resolution 4 K images and to examine the distribution of scale at great depths.

This technique was used to locate the areas of pie accumulation through a high magnification scan of the plate using the VHX-702 camera, VH-Z00 lens, and VH-Z100 lens.

Results and discussion

Experimental result

The deposit obtained without treatment is agglomerates of calcite, the thermodynamically hardest form of calcium carbonate.

During the experimental test, calcium, magnesium, carbonate, conductivity, and pH were monitored. Table 3 shows the experimental results obtained.

During the test, calcium concentration monitoring was performed by Ca^{2+} ion determination with ICP-OES spectroscopy. A decrease in calcium concentration was observed over time, as well as in conductivity, reflecting precipitation of calcium carbonate in the water on the "cold" side. Thus, the mass of dissolved calcium

Table 3. Cooling system water monitoring results during the experimental test.

Time (hours)	pH	Conductivity (µS/cm)	$[Ca^{2+}]$ (mg/L)	$[Mg^{2+}]$ (mg/L)
0	7.65	966.2	161	9.0
6	7.92	958.8	157.8	8.5
22	7.89	892	144.7	8.4
31	7.84	854.8	138.3	8.5
46	7.85	791	129.7	8.4
72	7.95	677.5	75.7	7.2

carbonate in the "cold" side water decreased as the exchanger was operated, as shown in Figure 4.

The mass of dissolved calcium carbonate in the water was estimated from the Ca^{2+} concentration by the following relation:

$$m_{CaCO_3} = [Ca^{2+}] \times \frac{M_{CaCO_3}}{M_{Ca}} \times 10^{-3} \times 100 \qquad (3)$$

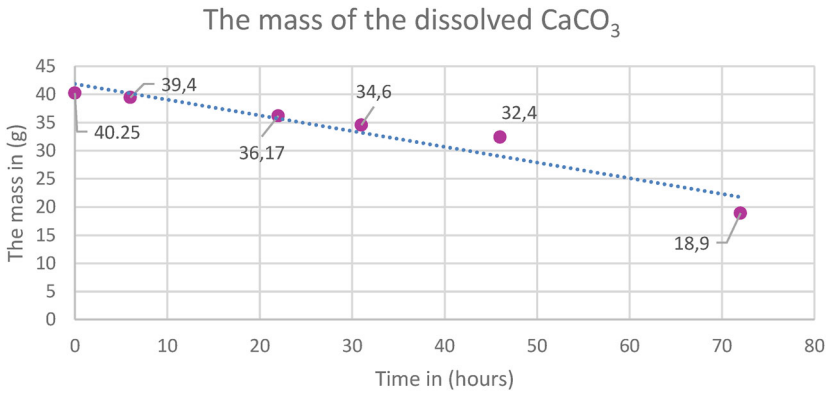

Figure 4. Variation in total mass of dissolved calcium carbonate in the cooling circuit during the test.

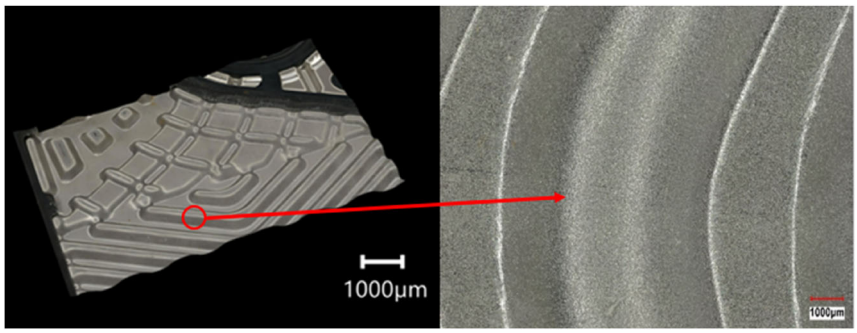

Figure 5. Exit of the first cold compartment of the exchanger after 3 days of operation (scan obtained with a magnification of ×20).

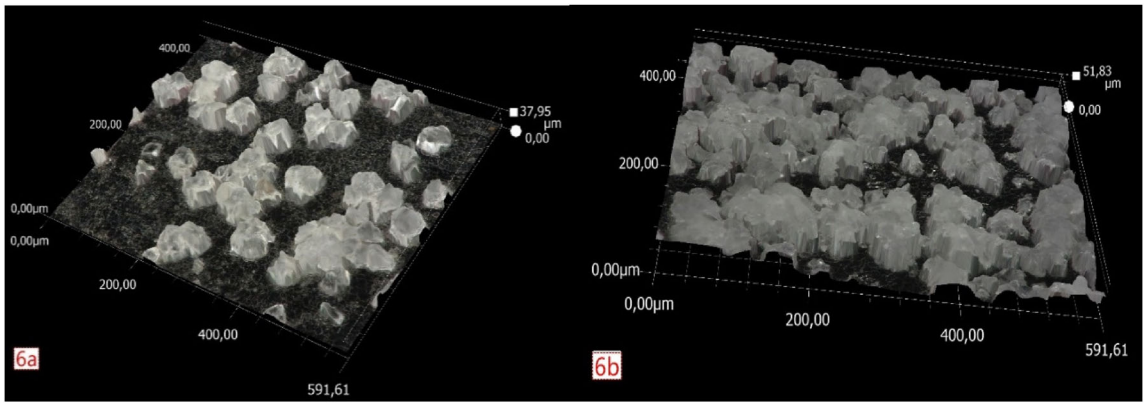

Figure 6. The height of the deposit at the inlet (a) and outlet (b) of the first cold compartment of the exchanger after 3 days of operation, 3D scan obtained with a magnification of ×500, with a 3D digital microscope.

The dismantling of the exchanger showed the presence of a homogeneous deposit between the two plates of the same compartment. The first comparative view between the plates that remained in contact with water for 72 h, illustrated the presence of a white deposit that makes the plates opaque, as shown in Figure 5.

The analysis of a plate embedded in the 3 D digital microscope for the purpose ensured the presence of the deposit, the identification of the homogeneity of scale on the surface of a single plate, and then measure the thickness of scale experimentally.

At the entrance of the plate, a thickness of 37 µm was observed (see Figure 6a), and at the exit of the plate, a thickness of 51.8 µm was observed (see Figure 6b).

Modeling results in Comsol, which includes a comprehensive set of features to study thermal designs and the effects of thermal loads (COMSOL n.d.), showed that the internal temperature of the fluid is non-homogeneous along with the exchanger (see Figures 7–9). At the inlet, the temperature was about 20 °C, and it increased progressively until it reached 40 °C at the outlet.

To confirm these simulation results by experiment, a surface fraction analysis by targeting was performed with a 3 D digital microscope on a plate from the first cold compartment of the exchanger scaled with calcium carbonate.

Fourteen areas with a surface of 3.16 mm^2 were scanned and analyzed with a 3 D digital microscope. At the entrance of the first cold

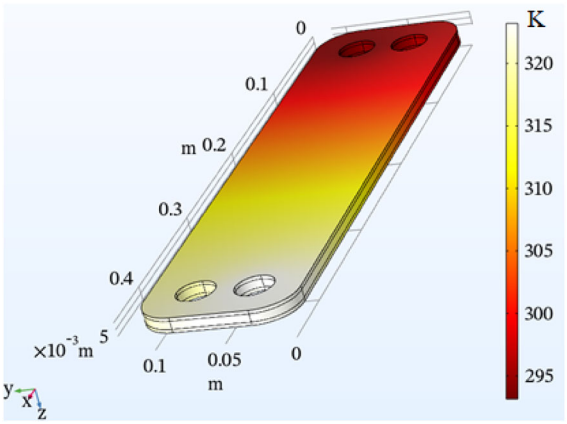

Figure 7. Temperature distribution along the plate.

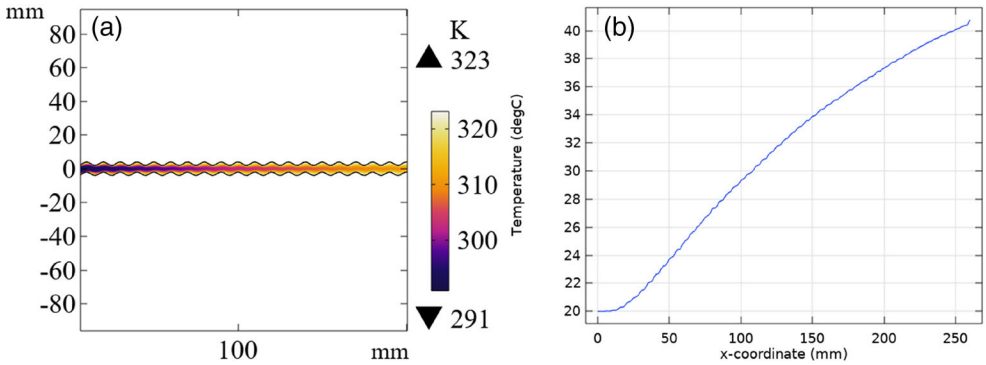

Figure 8. Temperature profile along the stacking of the two plates (a) with the temperature graph (b).

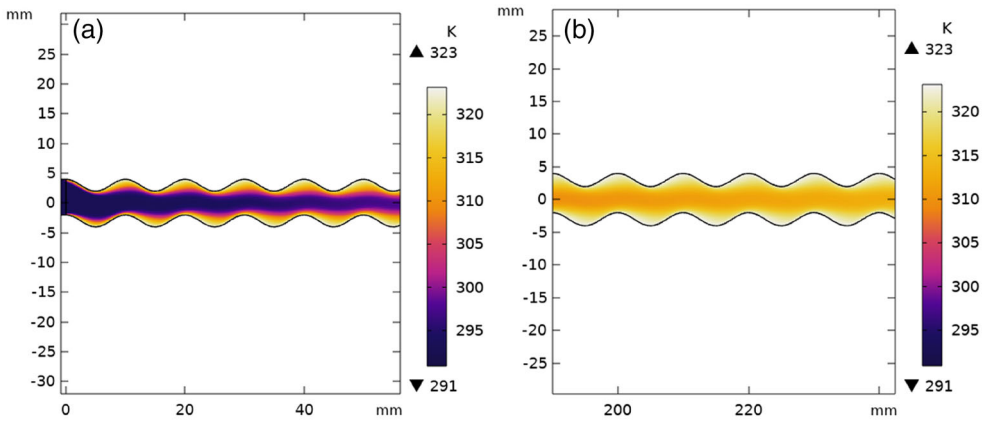

Figure 9. Temperature profiles at the inlet (a) and outlet (b) of the cold store.

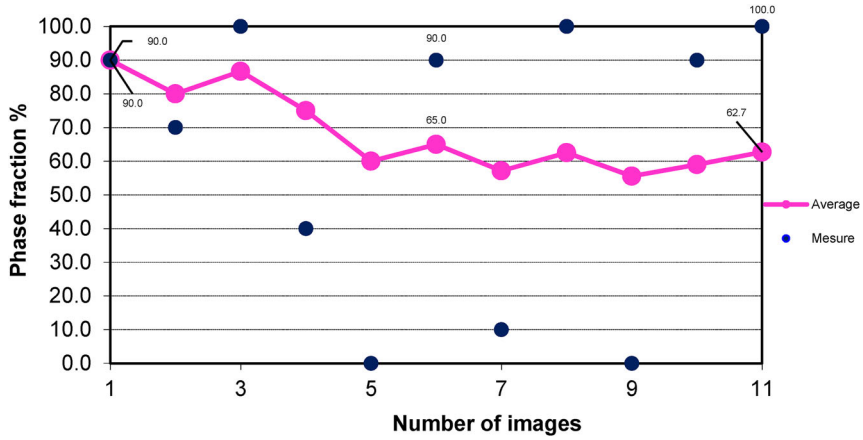

Figure 10. Surface fraction at the inlet of the first cold compartment of the exchanger after 3 days of operation.

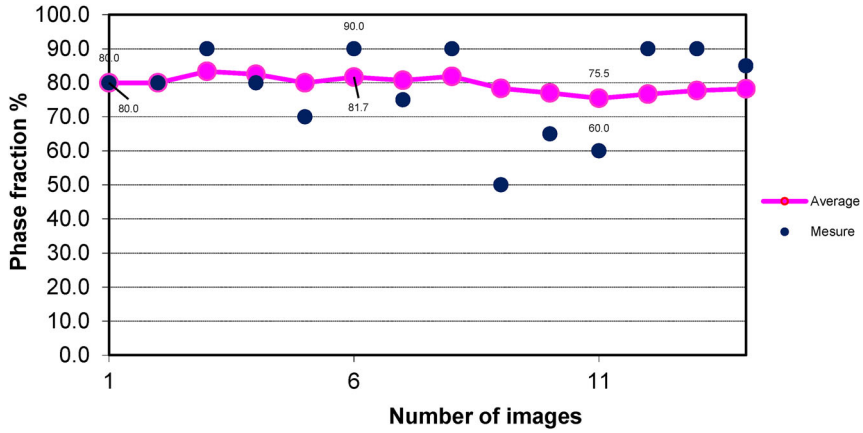

Figure 11. Surface fraction at the outlet of the first cold compartment of the exchanger after 3 days of operation.

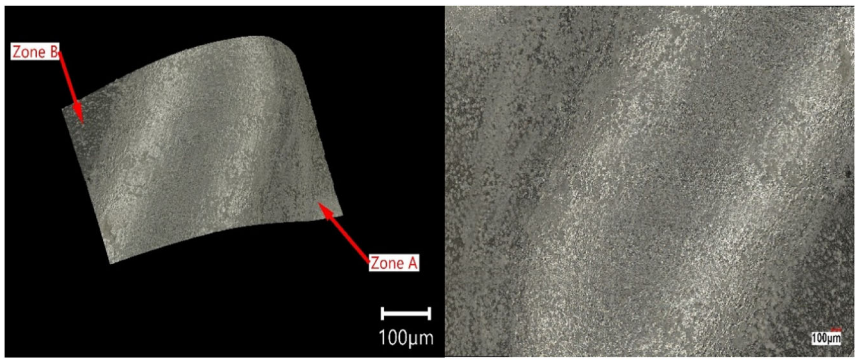

Figure 12. Distribution of calcium carbonate at the inlet of the first plate of the exchanger after 3 days of operation.

compartment, 62.7% of the surface was covered by crystals. At the exit of the same compartment, 78.2% of the surface was covered by crystals as shown in Figures 10 and 11. Modeling results show that for a single plate, the temperature was about 20 °C at the inlet, and it progressively increased until it reached 40 °C at the outlet. This explains the high percentage of crystals in the lower part of the exchanger compared to the upper part, with a difference of 15.5% of the surface covered with a deposit.

Scale refers to a hard deposit layer, which gradually accumulates on hot solid surfaces in contact with a mineral-rich fluid (Georgiou et al. 2018). Due to the different mineral contents and water treatment methods, the types of scale are different depending on the type of water heated, industrial or domestic water. Some of the most

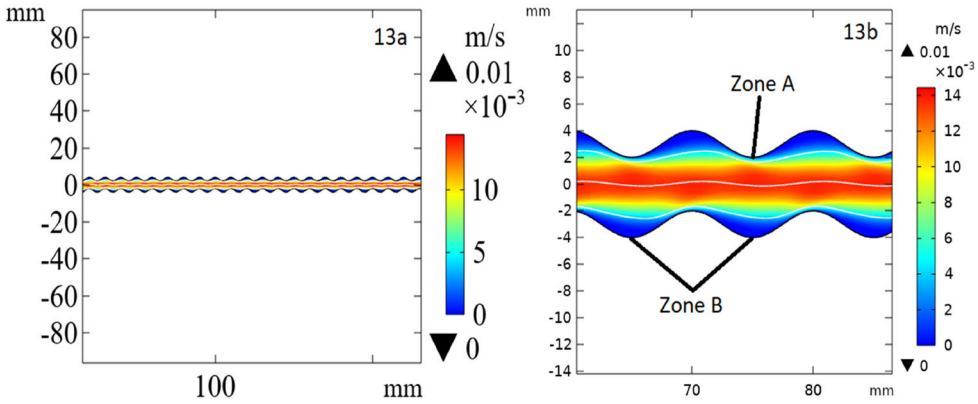

Figure 13. Flow velocity distribution between two plates.

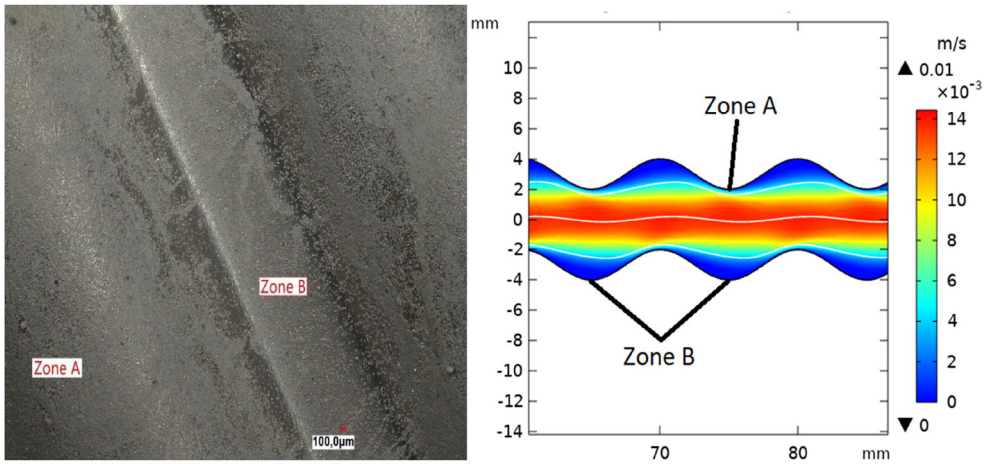

Figure 14. Calcium carbonate repair as a function of fluid flow rate in the different shapes of the center plate of the first cold compartment after 3 days of operation.

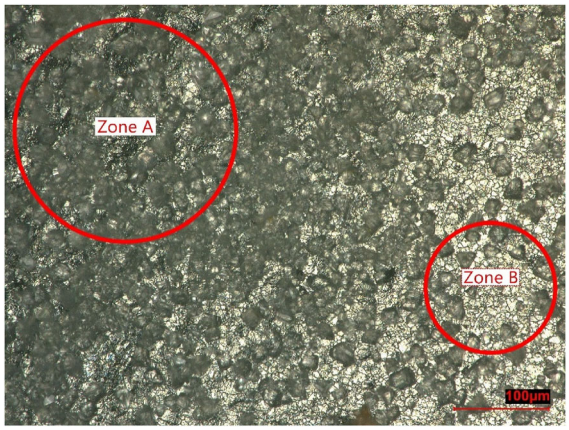

Figure 15. Distribution of calcium carbonate in the middle of the first compartment after 3 days of operation at magnification (×500).

common mineral ions found in scale are Ca^{2+} and Mg^{2+} (Teng et al. 2017). When hard water passes through heat exchange equipment, due to changes in pressure and solubility, and temperature, the mineral ions in the water react with bicarbonate ions and mineral deposits form on the surfaces of the heat exchange equipment (Pääkkönen et al. 2012). The scale causes the system to malfunction and even decreases the flow area of the water in the equipment (Frota et al. 2014), which affects the performance of heat transfer (Cho, Choi, and Drazner 1998).

In a study by Shengxian Cao et al. to investigate the effect of electromagnetic field on the same type of plates, when disassembling the exchanger, the authors noted that the thickness of the deposit is not homogeneous. For the cold compartment, it varies from 2 to 3 mm (Zhang et al. 2022).

On the other hand, Mr. Frota et al. in a study of an in-line cleaning technique to mitigate biofouling in a countercurrent operated exchanger, and the same type of plate in this paper to visualize the distribution of the organic deposit, noticed that the distribution of organic deposit is

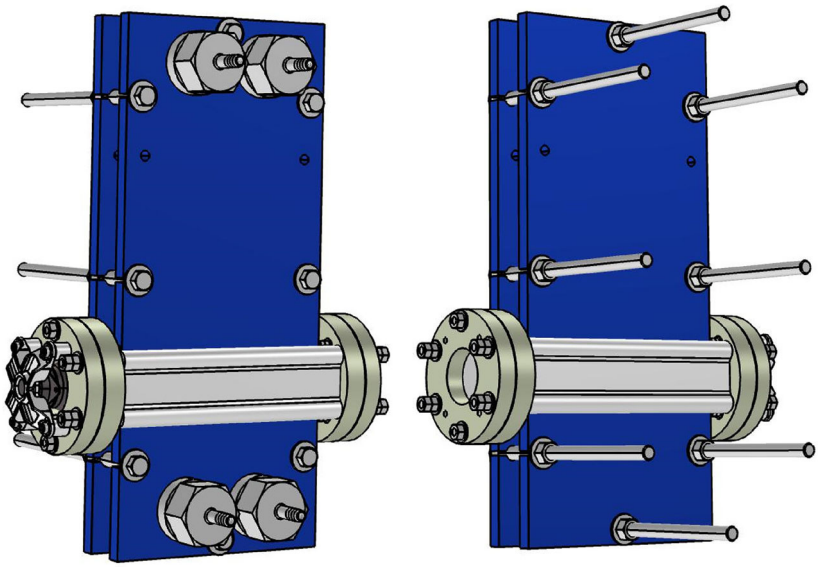

Figure 16. The location of the ultrasonic transducer after the limestone sensitivity analysis.

homogeneous (Frota et al. 2014), which is not like the case of a mineral deposit.

Calcium carbonate has an inverse solubility (Habibi and al. 2020), i.e., the more you heat scaling water, the more limestone is precipitated. Therefore, more crystallization of calcium carbonate was observed at the outlet compared to the inlet of the exchanger.

The Comsol modeling results were consistent with the results of the fraction of surface covered by limestone observed with the 3 D digital microscope.

Analysis of the plate grooves under the 3 D microscope at magnification (×250), showed that there are areas more susceptible to scale formation. As shown in Figure 12, in both areas A and B, less scale was seen compared to the central area.

When studying the velocity profile generated by Comsol on the plate model of the exchanger, the flow velocity was homogeneous along the plate. However, at a given dx, the presence of dead zones is noticed. As shown in Figure 13, the streamlines show that the velocity fields are not homogeneous, the fluid is quasi-stagnant between the splines, and it flows at a velocity close to 14 mm s^{-1} in the center of the gap between the two plates. In a study conducted by Alireza Jafari et al. in 2022 (Jafari, Sadeghianjahromi, and Wang 2022), based on the same approach, the authors experimentally and numerically studied brazed plate heat exchangers to identify the thermo-fluid characteristics of the exchanger.

By analyzing this area with a 3 D digital microscope with a magnification (×200) in Figure 14 and a magnification of the same area (×500) in Figure 15, it was found that calcium carbonate crystals are less present in the area B in which the water is stagnant.

However, the most scaled area was Zone A, which makes sense because the water in contact with these surfaces was constantly being renewed.

Conclusions

The major objective of this study is to justify the location of the ultrasonic transducer to inhibit calcium carbonate crystallization as much as possible.

The results of the two numerical modeling run under Comsol Multiphysics showed that the hottest zones are located at the bottom of the exchanger (cold fluid outlet, hot fluid inlet). These zones can therefore be described as more sensitive to the formation of calcium carbonate since the latter has an inverse solubility (the more one heats, the more one precipitates).

A complete examination of a scaled plate was performed using a 3 D digital microscope. Analysis of the plates with the 3 D digital microscope showed that the height of the deposit at the outlet was greater compared to the inlet.

Similarly, analysis of the surface fraction by targeting shows that 62% of the surface was covered with crystals at the cold inlet at the top of the exchanger. At the outlet of the same compartment, 78.2% of the surface was covered with crystals.

The comparison between the two studies shows that to further limit the formation of calcium carbonate inside the heat exchanger, it is necessary to place the ultrasonic system at the outlet of the cold fluid, in this case in the lower part of the exchanger, as shown in Figure 16.

Nomenclature

A	Exchange surface in m
C_p	The mass heat capacity in J. kg-1.K-1
h_{eq}	Global exchange coefficient in W.m-2.K-1
n	Unit vector
P	thermal power exchanged in W
ρ	The density in kg. m^{-3}
T	The temperature in °C
$T_{c,\ inlet}$	The inlet temperature of the cold liquid in °C
$T_{c,\ outlet}$	The outlet temperature of the cold liquid in °C
$T_{h,\ inlet}$	The inlet temperature of the hot liquid in °C
$T_{h,\ outlet}$	The outlet temperature of the hot liquid in °C
u	The fluid velocity field in $m.s^{-1}$

Authors' contributions

This study is part of the ExUS project and was directed by Dr. Hervé MUHR as thesis director. Dr. Marie LE PAGE MOSTEFA is co-director of the thesis. And the modeling under COMSOL Multiphysics, and the experiments and the scans of the plates with the 3 D digital microscope were carried out by Mrs Nihad Kamar, and finally, Mr. Pierre-Olivier JOST is the project leader.

Disclosure statement

The authors declare that they have no known competing financial interests or personal relationships that might appear to influence the work reported in this article.

Funding

The authors thank the Grand-Est region, BPI France, and the European Regional Development Fund for their financial support.

References

Al-Haj Ibrahim VH. 2012. Fouling in heat exchangers. MATLAB–A Fundamental Tool for Scientific Computing and Engineering Applications. Vol. 3. Edited by Vasilios N. Katsikis. doi:10.5772/46462

Brooks S, Roy R. 2022. Evaluation of a self-cleaning heat exchanger. Int J Heat Mass Transf. 191:122725. doi:10.1016/j.ijheatmasstransfer.2022.122725

Bulliard-sauret O. 2016. Thermiques Par Les Ultrasons En Convection Forc ' Ee Odin BULLIARD-SAURET Étude Expérimentale de l ' Intensification Des Transferts Thermiques Par Les Ultrasons En Convection Forcée.

Ch H. 2010. Modélisation de l ' Encrassement En Régime Turbulent Dans Un Échangeur de Chaleur à Plaques Avec Un Revêtement Fibreux Sur Les Parois Hamza Chérif Sadouk. To cite this version: HAL Id: Tel-00499251 Modélisation de l ' Encrassement En Régime Turbulent Dan.

Cho YI, Choi BG, Drazner BJ. 1998. Electronic anti-fouling technology to mitigate precipitation fouling in plate-and-frame heat exchangers. Int J Heat Mass Transfer. 41(17):2565–2571. doi:10.1016/S0017-9310(97)00347-5

COMSOL 2021. Echangeur de Chaleur à Plaques. https://www.comsol.fr/model/plate-heat-exchanger-2.

Module de Transfert de Chaleur. Analysez les effets thermiques avec le module de transfert de chaleur. https://www.comsol.fr/heat-transfer-module.

Shape optimization of a plate heat exchanger. https://www.comsol.fr/model/shape-optimization-of-.

De D, Grenoble DE, Legay M. 2012. Intensification Des Processus de Transfert de Chaleur Par Ultrasons, Vers Un Nouveau Type d ' Échangeur de Chaleur: L ' Échangeur Vibrant.

Epstein N. 1983. Thinking about heat transfer fouling: a 5×5 matrix. Heat Transfer Eng. 4(1):43–56. doi:10.1080/01457638108939594

Frota MN, Ticona EM, Neves AV, Marques RP, Braga SL, Valente G. 2014. On-line cleaning technique for mitigation of biofouling in heat exchangers: A case study of a hydroelectric power plant in Brazil. Exp Thermal Fluid Sci. 53:197–206. doi:10.1016/j.expthermflusci.2013.12.006

Georgiou D, Bendos D, Kalis M, Koutis C. 2018. Removal and/or prevention of limescale in plumbing tubes by a radio-frequency alternating electric field inductance device. J Water Process Eng. 22:34–40. doi:10.1016/j.jwpe.2017.12.013

Habibi H, Gan T-H, Legg M, Carellan I, Kappatos V, Tzitzilonis V, Selcuk C. 2016. An acoustic antifouling study in sea environment for ship hulls using ultrasonic guided waves. Int J Eng Tech Mgmt Res. 3(4):14–30. doi:10.29121/ijetmr.v3.i4.2016.59

Jafari A, Sadeghianjahromi A, Wang CC. 2022. Experimental and numerical investigation of brazed plate heat exchangers – A new approach. Appl Therm Eng. 200:117694. doi:10.1016/j.applthermaleng.2021.117694

Jakati RS, Balavalad KB, Sheeparamatti BG. 2016. Comparative analysis of different micro-pressure sensors using Comsol multiphysics. In 2016 International Conference on Electrical, Electronics, Communication, Computer and Optimization Techniques (ICEECCOT), 355–60.

Zhang K, Van Le Q, Tosiriwatanapong T, Singhatanadgit W. 2018. Bioactive glass coated zirconia for dental implants. J Compos Compound. 2(2):35–43.doi:10.29252/jcc.2.1.2

Martins GSM, Santiago RS, Beckedorff LE, Possamai TS, Oba R, Oliveira JLG, de Oliveira AAM, Paiva KV. 2022. International journal of pressure vessels and piping structural analysis of gasketed plate heat exchangers American society of mechanical engineers. Int J Press Vessels Pip. 197:104634. doi:10.1016/j.ijpvp.2022.104634

Müller-Steinhagen H. 2011. Heat transfer fouling: 50 years after the Kern and Seaton model. Heat Transfer Engineering. 32(1):1–13. doi:10.1080/01457632.2010.505127

Pääkkönen TM, Riihimäki M, Simonson CJ, Muurinen E, Keiski RL. 2012. Crystallization fouling of $CaCO_3$—analysis of experimental thermal resistance and its uncertainty. International Journal of Heat and Mass Transfer. 55(23-24):6927–6937. doi:10.1016/j.ijheatmasstransfer.2012.07.006

Pau UDE, Des ET, Adour PDEL, Cazenave F. 2019. "Modélisation et Simulation de l'encrassement Des Échangeurs de Chaleur Pour Eaux Géothermales.".

Sakkaki M, Sadegh Moghanlou F, Parvizi S, Baghbanijavid H, Babapoor A, Shahedi Asl M. 2020. Phase change materials as quenching media for heat treatment of 42CrMo4 steels. J Cent South Univ. 27(3):752–761. doi:10.1007/s11771-020-4328-8

Singh S, Kaler RS. 2018. Performance analysis of evanescent wave absorption plasmonic optical sensor with COMSOL FEM method simulation. Procedia Comput Sci. 125:376–381. doi:10.1016/j.procs.2017.12.049

Tajik B, Abbassi A, Saffar-Avval M, Abdullah A, Mohammad-Abadi H. 2013. Heat transfer enhancement by acoustic streaming in a closed cylindrical enclosure filled with water. Int J Heat Mass Transfer. 60(1):230–235. doi:10.1016/j.ijheatmasstransfer.2012.12.066

Teng KH, Kazi SN, Amiri A, Habali AF, Bakar MA, Chew BT, Al-Shamma'a A, Shaw A, Solangi KH, Khan G, et al. 2017. Calcium carbonate fouling on double-pipe heat exchanger with different heat exchanging surfaces. Powder Technol. 315:216–226. doi:10.1016/j.powtec.2017.03.057

Thackery PA, Thackery PA. 1980. The cost of fouling in heat exchange plant.

Wu T, Ro PI. 2005. Heat transfer performance of a cooling system using vibrating piezoelectric beams. J Micromech Microeng. 15(1):213–220. doi:10.1088/0960-1317/15/1/030

Zhang Y, Cao S, Wang Y, Wang G, Sun T 2022. Application of Alternating Electric Field Scale Inhibition Device in Heat Exchange Station. Int J Heat Mass Transf. 185:122321. doi:10.1016/j.ijheatmasstransfer.2021.122321